

# Bone Ridge Patterning during Musculoskeletal Assembly Is Mediated through SCX Regulation of *Bmp4* at the Tendon-Skeleton Junction

Einat Blitz,<sup>1</sup> Sergey Viukov,<sup>1</sup> Amnon Sharir,<sup>1,2</sup> Yulia Schwartz,<sup>1</sup> Jenna L. Galloway,<sup>3</sup> Brian A. Pryce,<sup>4</sup> Randy L. Johnson,<sup>5</sup> Clifford J. Tabin,<sup>3</sup> Ronen Schweitzer,<sup>4</sup> and Elazar Zelzer<sup>1,\*</sup>

<sup>1</sup>Department of Molecular Genetics, Weizmann Institute of Science, Rehovot 76100, Israel

<sup>2</sup>Koret School of Veterinary Medicine, Faculty of Agricultural, Food and Environmental Quality Sciences, The Hebrew University of Jerusalem, Rehovot 76100, Israel

<sup>3</sup>Department of Genetics, Harvard Medical School, Boston, MA 02115, USA

<sup>4</sup>Shriners Hospital for Children, Research Division, Portland, OR 97239, USA

<sup>5</sup>Department of Biochemistry and Molecular Biology, University of Texas, MD Anderson Cancer Center, Houston, TX 77030, USA

\*Correspondence: eli.zelzer@weizmann.ac.il

DOI 10.1016/j.devcel.2009.10.010

## SUMMARY

During the assembly of the musculoskeletal system, bone ridges provide a stable anchoring point and stress dissipation for the attachment of muscles via tendons to the skeleton. In this study, we investigate the development of the deltoid tuberosity as a model for bone ridge formation. We show that the deltoid tuberosity develops through endochondral ossification in a two-phase process: initiation is regulated by a signal from the tendons, whereas the subsequent growth phase is muscle dependent. We then show that the transcription factor scleraxis (SCX) regulates *Bmp4* in tendon cells at their insertion site. The inhibition of deltoid tuberosity formation and several other bone ridges in embryos in which *Bmp4* expression was blocked specifically in *Scx*-expressing cells implicates BMP4 as a key mediator of tendon effects on bone ridge formation. This study establishes a mechanistic basis for tendon-skeleton regulatory interactions during musculoskeletal assembly and bone secondary patterning.

## INTRODUCTION

The musculoskeletal system has played a pivotal role in the evolutionary success of vertebrates by providing their bodies with form, stability, and mobility. The proper functionality of the musculoskeleton relies on precise assemblage and tight coordination among its components: skeletal tissue (bone, cartilage, and joints), muscles, and tendons. The research of the musculoskeleton as an integrated system has been scarce. As a result, little is known about the regulatory interactions among its three components during its development.

The appendicular skeleton forms by endochondral ossification. During this process, cartilaginous templates are replaced by bone and bone marrow. The replacement of cartilage by ossified bone and its longitudinal growth are regulated by the growth

plate. It is located near the ends of long bones and composed of chondrocytes that undergo a well-defined and highly controlled differentiation program (Karsenty and Wagner, 2002; Olsen et al., 2000).

Several signaling pathways are known to regulate chondrocyte differentiation, notably bone morphogenetic proteins (BMPs), members of the transforming growth factor  $\beta$  (TGF  $\beta$ ) superfamily (Pogue and Lyons, 2006). BMP ligands bind to their specific serine/threonine kinase receptor and initiate a signaling cascade leading to the phosphorylation of transcription regulators, the Smad proteins (Smad 1/5/8). The P-Smad 1/5/8 then translocate into the nucleus and activate the transcription of various target genes (Massague et al., 2005). The ability of BMPs to induce ectopic cartilage suggests an involvement of these factors in chondrogenesis (Reddi and Huggins, 1972; Urist, 1965; Wozney et al., 1988). Indeed, abrogation of the expression of both BMP type 1 receptors, *Bmpr1a* and *Bmpr1b*, in chondrocytes has demonstrated the role of BMPs in chondrocyte proliferation, survival, and differentiation (Yoon et al., 2005).

While the longitudinal growth of bone has attracted most of the attention, a secondary patterning process also exists. Different bones grow protrusions of varying shapes and sizes on their surface, structures that are significant in the final and specific design of each bone. Bone protrusions are divided into two groups: articular and nonarticular. Examples of articular eminences are found in the heads of the humerus and femur. Nonarticular eminences are located along the bone shaft and termed according to their form. Thus, a rough elevation that stretches along the surface is termed a ridge or crest, whereas a broad, rough, irregular ridge is called a tuberosity.

Bone ridges play a fundamental role in the functionality of the musculoskeletal system, providing a stable anchoring point for muscles, inserted to the skeleton via tendons. Most of the mechanical load applied to the skeleton, generated by muscle contraction and transduced by tendons, encounters bone ridges first. These structures then absorb and dissipate some of the stress concentrated at the hard-soft tissue interface, thereby diminishing the risk of avulsion fractures (Biewener et al., 1996; Benjamin et al., 2002).

Interestingly, despite their necessity, the cellular and molecular mechanisms that regulate bone ridge patterning and development are mostly unknown. Notwithstanding, several studies performed in different systems including bone transplantation, immobilized chick embryos, and mice that lack functional musculature (Hamburger, 1938, 1939, 1940; Hall and Herring, 1990; Hosseini and Hogg, 1991; Pai, 1965a; Rot-Nikcevic et al., 2006; Tremblay et al., 1998) have suggested the contribution of mechanical load created by muscle contraction to the formation of bone ridges. In the limb, muscle progenitors develop in close proximity to tendon precursors and the morphogenesis of these two tissues is tightly coupled, both spatially and temporally (Kardon, 1998; Schweitzer et al., 2001). Surgical manipulations in chick embryos and genetic analyses in mice have shown that limb tendon development can be initiated in the absence of muscles; however, later in development, tendon maintenance requires the presence of muscles (Bonnin et al., 2005; Brent et al., 2005; Edom-Vovard et al., 2002; Kardon, 1998; Kiely and Chevallier, 1979; Schweitzer et al., 2001).

Unlike the musculature and the skeleton, the molecular aspects of tendon development have only recently begun to be uncovered. The finding that scleraxis (SCX), a bHLH transcription factor, is expressed in progenitors and cells of all tendinous tissues and regulates their differentiation (Cserjesi et al., 1995; Murchison et al., 2007; Schweitzer et al., 2001) provides a molecular entry point into tendon development. Despite these advances, little is known about the interaction between tendon and cartilage cells in the forming limb.

As a model for studying the regulatory role of interactions among different tissues during musculoskeletal assembly, we investigated the development of a bone ridge named the deltoid tuberosity (referred to hereafter as DT). We show a temporally regulated and coordinated contribution of both tendons and muscles to DT development, as tendons regulate tuberosity initiation and muscles control its growth. We then describe a molecular pathway that mediates a crosstalk between cartilage and tendons whereby BMP4, produced by tendon cells at the insertion site under the regulation of SCX, regulates bone ridge formation.

## RESULTS

### DT Develops through Endochondral Bone Formation

Very little is known about the formation of bone ridges. As a model for studying the development of these structures we chose the DT, a bone ridge located on the shaft of the humerus that exhibits a well-defined morphology.

To document DT development, we stained skeletons of E14.5–E18.5 wild-type (WT) embryos with Alizarin red and Alcian blue. At E14.5, we observed the emergence of the tuberosity from the lateral aspect of the proximal third of the humerus (Figure 1A). As DT development proceeded, it maintained its growth; concomitantly, it underwent ossification, except for a cartilaginous part at its tip (Figures 1B and 1C).

To study the cellular mechanism by which the DT forms, we next analyzed histologically sagittal and transverse sections of E13.5–E18.5 WT limbs. At E13.5, a group of cells with a distinctive appearance emerge from the proximal epiphysis of the humerus, indicating the initiation of DT formation (Figure 1D).

At E14.5, these cells appeared similar to chondrocytes in the proliferative zone of the humerus primary growth plate (Figures 1E and 1H). At later stages (E16.5), we observed prehypertrophic and hypertrophic chondrocytes (Figures 1F and 1I). Their emergence was followed by blood vessel invasion and by E18.5 (Figures 1G and 1J) bone formation was clearly observed. This sequence of events suggests that the DT develops through endochondral ossification.

The hallmark of endochondral ossification is the formation of a growth plate. To validate our hypothesis that the tuberosity is formed by endochondral ossification, we examined the expression of growth plate markers in E16.5 WT embryos (Figures 1K–1O). The markers we analyzed included collagen type II alpha 1 (*Col2a1*), a marker for resting and proliferating chondrocytes, Indian hedgehog (*Ihh*) and parathyroid hormone-related peptide receptor (*PTHRPR*), markers for prehypertrophic chondrocytes, and collagen type X alpha 1 (*Col10a1*), a marker for hypertrophic chondrocytes (Kronenberg, 2003). The differential expression of these markers in the developing DT (Figure 1L–1O) strongly supports our conclusion that the tuberosity develops by endochondral ossification.

To determine the growth direction of the tuberosity growth plate, we examined cell proliferation by analyzing BrdU incorporation into cells of the DT. In E16.5 WT embryos, we detected a group of proliferating chondrocytes at the tip of the DT (Figure 1P). This result indicates that the direction of DT growth is different from that of the humerus primary growth plate.

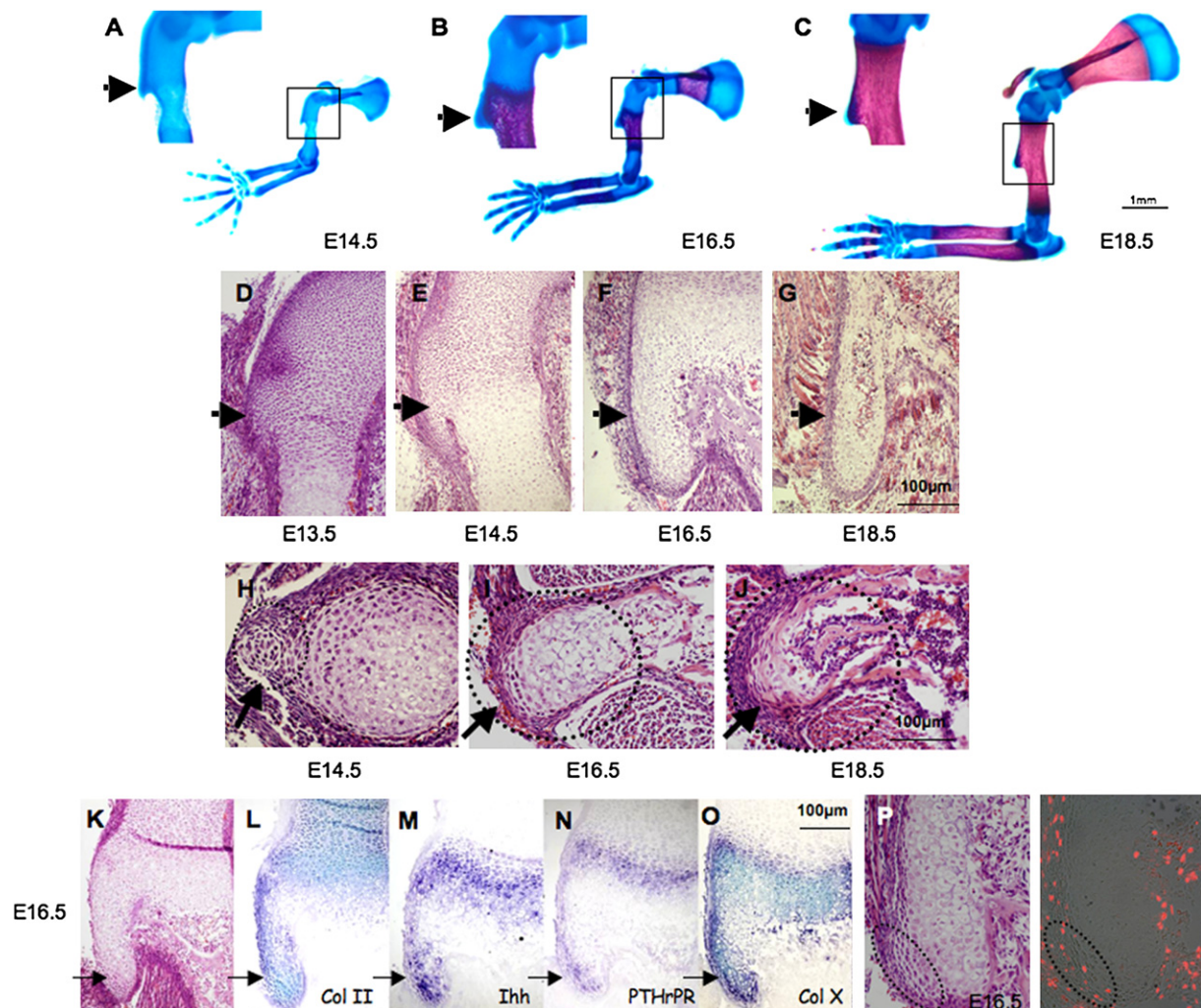
### Tuberosity Initiation Is Muscle Independent

Studies performed over the last century have established the contribution of mechanical load created by muscle contraction in the formation of bone ridges (Hamburger, 1938, 1939, 1940; Hall and Herring, 1990; Hosseini and Hogg, 1991; Pai, 1965a; Rot-Nikcevic et al., 2006; Tremblay et al., 1998). However, all those studies document bone ridge development in ossified bones at relatively advanced stages of skeleton development. Our finding that the DT emerges as a cartilaginous template at an earlier stage of skeletogenesis prompted us to study the role of the musculature in regulating the initial stages of DT development.

We examined the skeletons of two strains of mutant mice with muscular defects. The splotch delayed mutant (*Sp<sup>d</sup>*) mice harbor a naturally occurring point mutation in the *Pax3* gene. Homozygous *Sp<sup>d</sup>* embryos lack all limb musculature due to a defect in the migration of muscle progenitor cells to the developing limb (Dickie, 1964; Franz et al., 1993). The second mouse strain, which carries the naturally occurring autosomal recessive mutation muscular dysgenesis (*mdg*), lacks excitation-contraction coupling, leading to the absence of skeletal muscle contractility (Pai, 1965a, 1965b).

First, we analyzed skeletal preparations of forelimbs from E18.5 homozygous *Sp<sup>d</sup>* and *mdg* embryos. Consistently with previous findings, these skeletons lacked the DT (Figures 2A and 2B) (Pai, 1965a; Rot-Nikcevic et al., 2006; Tremblay et al., 1998). While bone ridge development was dramatically impaired, a mild effect on the humerus longitudinal growth and ossification was also observed at E18.5 (data not shown).

To determine the influence of the musculature on tuberosity initiation, we examined embryonic skeletons at E14.5, 1 day after DT development initiates. Surprisingly, the DT was present in

**Figure 1. Developmental Analysis of the DT**

(A–P) Black arrows indicate DT.

(A–C) Skeletal preparations of E14.5, E16.5, and E18.5 WT embryos (the boxed areas of the DT are enlarged on the left).

(D–J) Histological sagittal (D–G) and transverse (H–J) sections through the DT of E13.5–E18.5 WT mice (dotted circles indicate DT area).

(K–O) Tuberosity cell differentiation is demonstrated by the expression of growth plate markers.

(K) Histological sagittal section through the DT of E16.5 WT mice.

(L–O) In situ hybridization analysis of DT sagittal sections from E16.5 WT mice, using anti-sense complementary RNA probes for collagen II (Col II), Indian hedgehog (Ihh), parathyroid hormone-related peptide receptor (PTHrPR), and collagen X (Col X) mRNA.

(P) BrdU incorporation in E16.5 WT mice; dotted circles indicate tuberosity tip.

homozygous *Sp<sup>d</sup>* and *mdg* embryos (Figures 2C and 2D). Additionally, chondrocytes in the DT of the *mdg* mutant mice continued their differentiation to hypertrophy (Figures 2E–2I); however, they failed to maintain normal proliferation rate (see Figure S2 available online).

These results demonstrate that DT development is a biphasic process, consisting of initiation and growth phases. The initiation phase is muscle-independent, whereas the subsequent growth phase depends on muscle contraction.

#### Tendons Are Necessary for Bone Ridge Formation

Intrigued by the biphasic nature of DT development, we sought to identify the trigger of the initiation phase. Recent reports

have demonstrated the lack of DT in embryos where the expression of *Tgf-β* receptor II (*Tgf-βRII*) was conditionally targeted in limb mesenchyme, using the *Prx1-Cre* as a deleter mouse (*Prx1-Tgf-βRII*) (Seo and Serra, 2007; Spagnoli et al., 2007; Baffi et al., 2004; Logan et al., 2002). Recently, we showed that TGF-β signaling was essential for tendon development, as in the *Prx1-Tgf-βRII* embryos tendons and ligaments were lost (Pryce et al., 2009). In light of this evidence and given the biphasic nature of tuberosity formation, we decided to use the *Prx1-Tgf-βRII* embryos to study the role of tendon cells in DT initiation.

First, to verify the loss of tendons at the attachment site we examined the expression of scleraxis (SCX), a marker for

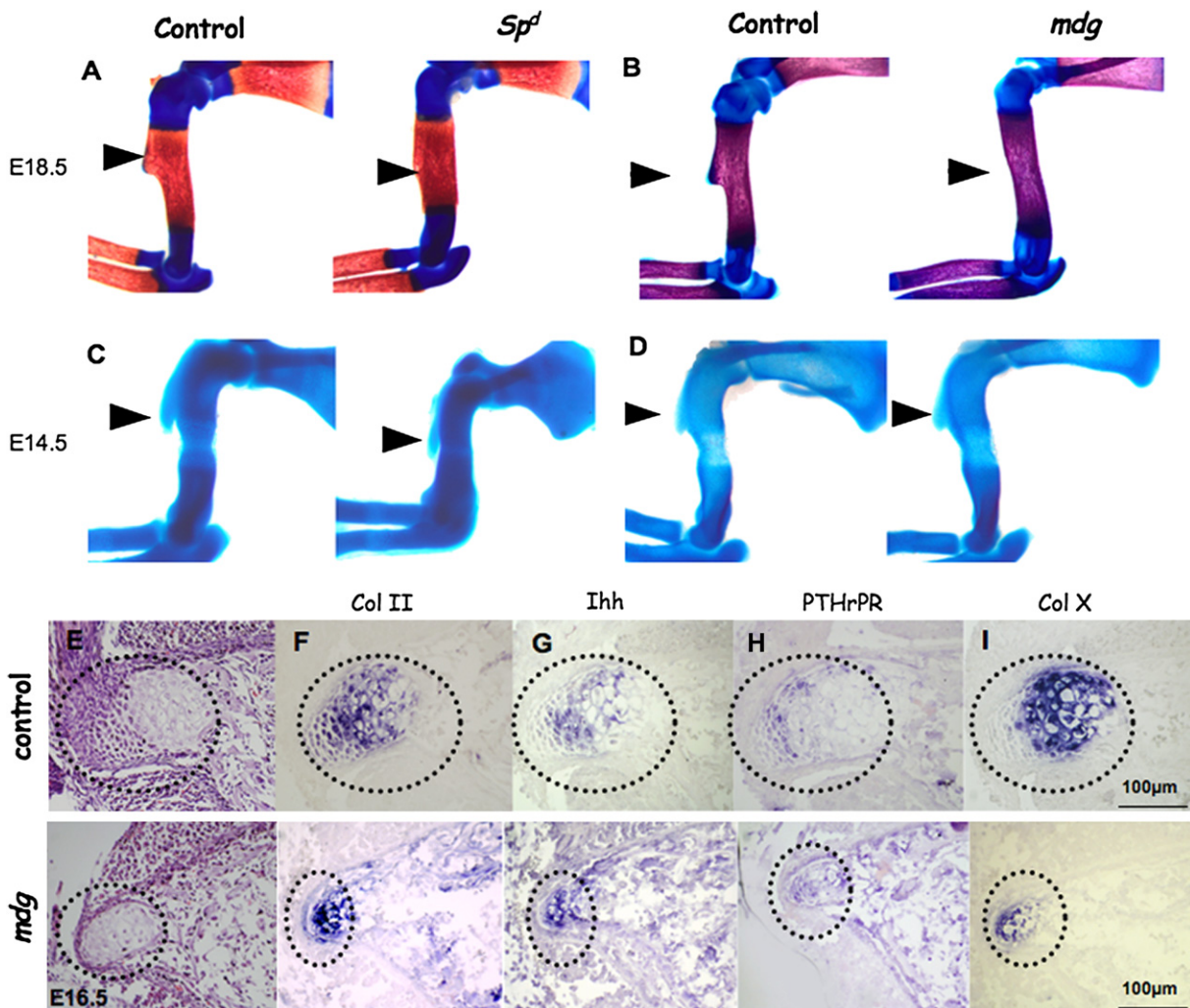


**Figure 2. Bone Ridge Development Is Disrupted in Mice with Defective Musculature**

(A–D) Forelimbs of E18.5 (A and B) and E14.5 (C and D) control, *Spd/Spd*, and *mdg/mdg* mice stained with Alcian blue and Alizarin red. Black arrows indicate DT.

(E–I) Expression of growth plate markers in paralyzed embryos (dotted circles indicate DT area).

(E) Histological transverse sections of control and *mdg* mutant E16.5 tuberosity.

(F–I) *In situ* hybridization analysis of DT transverse sections from E16.5 control and *mdg* mice using anti-sense complementary RNA probes for collagen II (Col II), Indian hedgehog (Ihh), parathyroid hormone-related peptide receptor (PTHrPR), and collagen X (Col X) mRNA.

tendons, in embryos homozygous for *floxed-Tgf-βRII* and heterozygous for *Prx1-Cre* alleles (*Prx1-Tgf-βRII*) and embryos heterozygous for *floxed-Tgf-βRII* and *Prx1-Cre* alleles (control). As expected, no *Scx* expression could be observed in *Prx1-Tgf-βRII* forelimbs (Figures 3A and 3B). Next, we studied DT initiation in the *Tgf-βRII*-ablated limbs. Skeletal preparations of E14.5 *Prx1-Tgf-βRII* forelimbs lacked DT initiation (Figure 3C). These results strongly imply that tendons are necessary for the initial signal that induces the formation of the DT.

#### SCX Is Necessary for DT Initiation

Our finding that tendons are necessary for DT initiation prompted us to screen for molecules that mediate this interaction. We previously showed that *Scx*<sup>−/−</sup> newborn mice lacked the tuberosity and suggested that the phenotype might be attributed to a failure in the transmission of mechanical load from muscles

to the skeleton, due to tendon abnormality (Murchison et al., 2007). Having found an involvement of tendons in the induction of DT formation, we postulated that SCX might regulate tuberosity initiation. SCX is essential for tendon differentiation and in *Scx*<sup>−/−</sup> mice—some of the tendons appeared rudimentary and others were completely missing (Murchison et al., 2007). Therefore, we first had to verify that tendons formed at the *Scx*<sup>−/−</sup> humerus attachment site, prior to DT initiation. To this end, we crossed the *ScxGFP* transgenic tendon reporter mouse into the *Scx*<sup>−/−</sup> background (Pryce et al., 2007). In sagittal sections through the humeri of E13.5 embryos, tendons attaching at the initiation site of the DT, visualized as *ScxGFP*-positive cells, were observed in both *Scx*<sup>+/−</sup> (control) and *Scx*<sup>−/−</sup> mutants (Figure 3D). Thus, despite the presence of tendon cells at the humerus insertion site of *Scx*<sup>−/−</sup> mutant embryos, these embryos lacked DT initiation (Figures 3E and 3F).

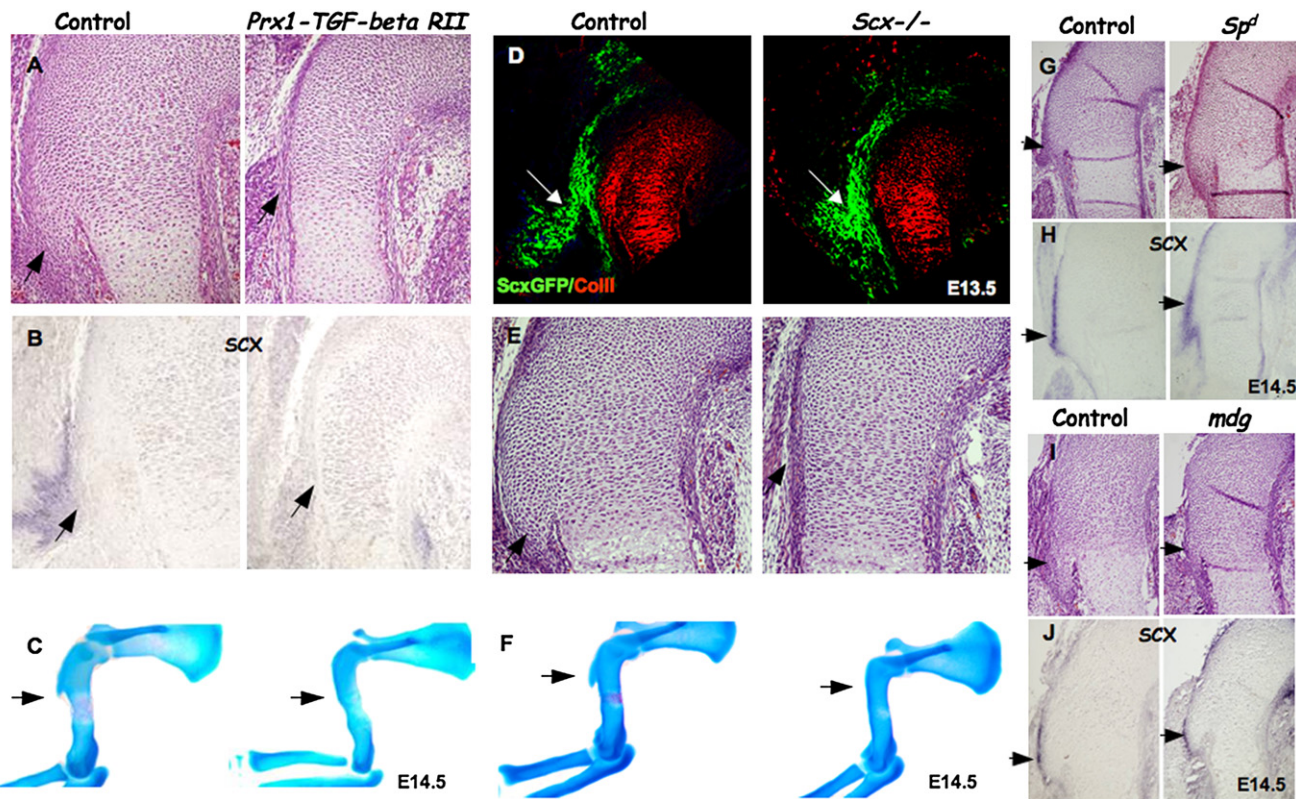


**Figure 3. Tendons Regulate DT Initiation through Scleraxis**

(A–J) Black arrows point at DT.

(A and B) Detection of scleraxis expression as an indication for tendon formation in *Prx1-Tgf-βRII* embryos.

(A) Histological sagittal sections through the humeri of control and *Prx1-Tgf-βRII* mice.

(B) In situ hybridization of sections through the humeri of control and *Prx1-Tgf-βRII* embryos at E14.5, using *Scx* probe.

(C) Skeleton preparation of control and *Prx1-Tgf-βRII* mice.

(D) Sagittal sections through the humeri of control and *Scx*<sup>−/−</sup> embryos carrying the *ScxGFP* reporter and counterstained with anti-collagen II antibody. White arrows mark tendon attachment site and the presumable initiation site of the DT (green, tendon; red, cartilage).

(E and F) Detection of DT by (E) histological sagittal sections through the humerus and (F) skeleton preparation of E14.5 *Scx*<sup>−/−</sup> mutant.

(G–J) *Scx* expression in control, muscle-less (homozygous *Spd*), and paralyzed (*mdg*) mice.

(G and I) Histological sagittal sections through the humeri of control, *Spd*, and *mdg* mutant mice.

(H and J) In situ hybridization through the humeri of control and *Spd* and *mdg* embryos at E14.5, using *Scx* probe.

If *Scx* is required for DT initiation, it should be expressed in the *Spd* and *mdg* mutant mice, which display normal initiation. As expected, *Scx* was expressed at the initiation site in both strains, similarly to control mice (Figures 3G–3J). These results implicate SCX as a key molecule in the regulation of DT initiation by tendons.

#### Bmp4 Expression in Tendons Is Regulated by SCX

The regulation of DT initiation by SCX must operate through a cell-nonautonomous mechanism, since *Scx* expression is restricted to tendons. Because SCX is a transcription factor, we performed a miniscreen of candidate molecules to identify secreted factors that act downstream to SCX and mediate the nonautonomous initiation signal from the tendons to the skeleton. We detected bone morphogenetic protein 4 (*Bmp4*) expression in tendon cells at the attachment site at E13.5, making it a likely candidate to initiate tuberosity formation (Figures 4A–4C). Moreover, *Bmp4* expression in tendons was colocalized with *Scx* expression, mainly at the attachment site

(Figures 4A and 4C). The coexpression of *Bmp4* and *Scx* was also observed in other tendon-cartilage intersections, such as the elbow joint (Figure 4B).

The coexpression of *Scx* and *Bmp4* in tendon-cartilage intersections prompted us to examine whether SCX is necessary for *Bmp4* expression in tendons. The specific loss of *Bmp4* expression at the tendon insertion site of *Scx*<sup>−/−</sup> embryos implied that SCX acts upstream to BMP4 in tendon cells (Figures 4C and 4D).

#### SCX Regulates the Transcription of *Bmp4*

The coexpression of *Scx* and *Bmp4* and the reduction in *Bmp4* expression in tendon-cartilage intersection point of *Scx*<sup>−/−</sup> mice led us to determine whether or not SCX regulates the transcription of *Bmp4*. First, we examined the ability of *Scx* overexpression to induce an increment in *Bmp4* expression in cell culture, by either transiently or stably transfecting *Scx* into C3H10T1/2 cells. In both cases, quantitative RT-PCR revealed an elevation in *Bmp4* expression in *Scx*-transfected cells (Figures 4E and 4F). To determine whether or not the increased

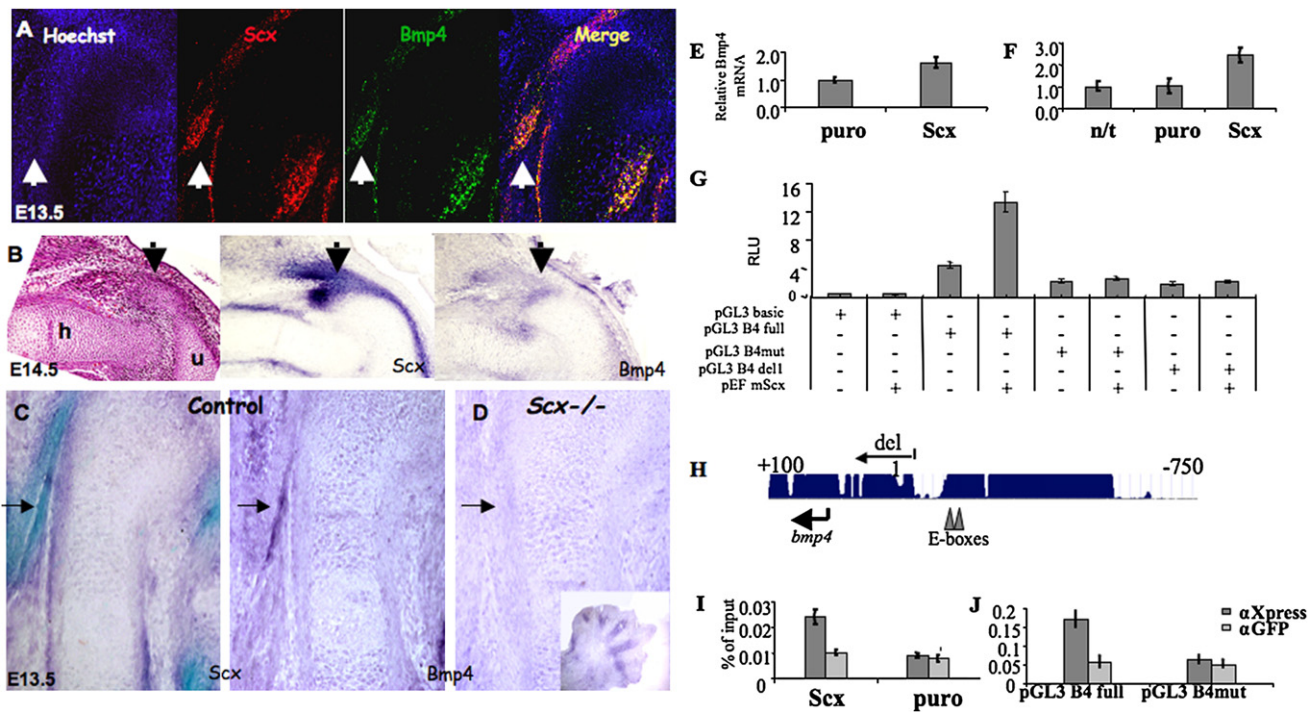


**Figure 4. BMP4 Acts Downstream of Scleraxis**

(A) Double fluorescent in situ hybridization of DT sagittal sections from E13.5 WT mice, using anti-sense complementary RNA probes for Scx and *Bmp4*; white arrows mark tendon insertion site.

(B) In situ hybridization of forelimb joint sagittal sections from E14.5 WT mice, using anti-sense complementary RNA probes for Scx and *Bmp4*.

(C and D) In situ hybridization analysis of sagittal sections of humeri at E13.5, using anti-sense complementary RNA probes for Scx and *Bmp4*; black arrows mark tendon insertion site.

(E and F) qRT-PCR analysis of *Bmp4* mRNA levels in C3T1/2H10 cells transiently (E) or stably (F) transfected with Scx. Stable cells (F) were transfected with empty vector or Scx and passed selection or kept in culture without transfection (n/t).

(G) Luciferase activity in HeLa cells transfected with indicated plasmids: pGL3 B4 full,  $-750$ – $+100$  promoter region; B4 mut, promoter region with E-boxes mutated; del1 as in (H).

(H) A diagram of *Bmp4* gene region surrounding the transcription start site showing E-boxes and the deletion used in (G).

(I) ChIP analysis of Scx and puro.

(J) Plasmid IP performed on cells cotransfected with the intact *Bmp4* promoter (pGL3B4 full) or *Bmp4* promoter with 3-nucleotide substitutions ablating the E-boxes (pGL3B4 mut) and Scx-expressing vector.

In (I) and (E), qRT-PCR was performed with primers specific to the E-boxes region of the *Bmp4* promoter ( $n = 3$ ). Error bars represent the standard deviation from the mean.

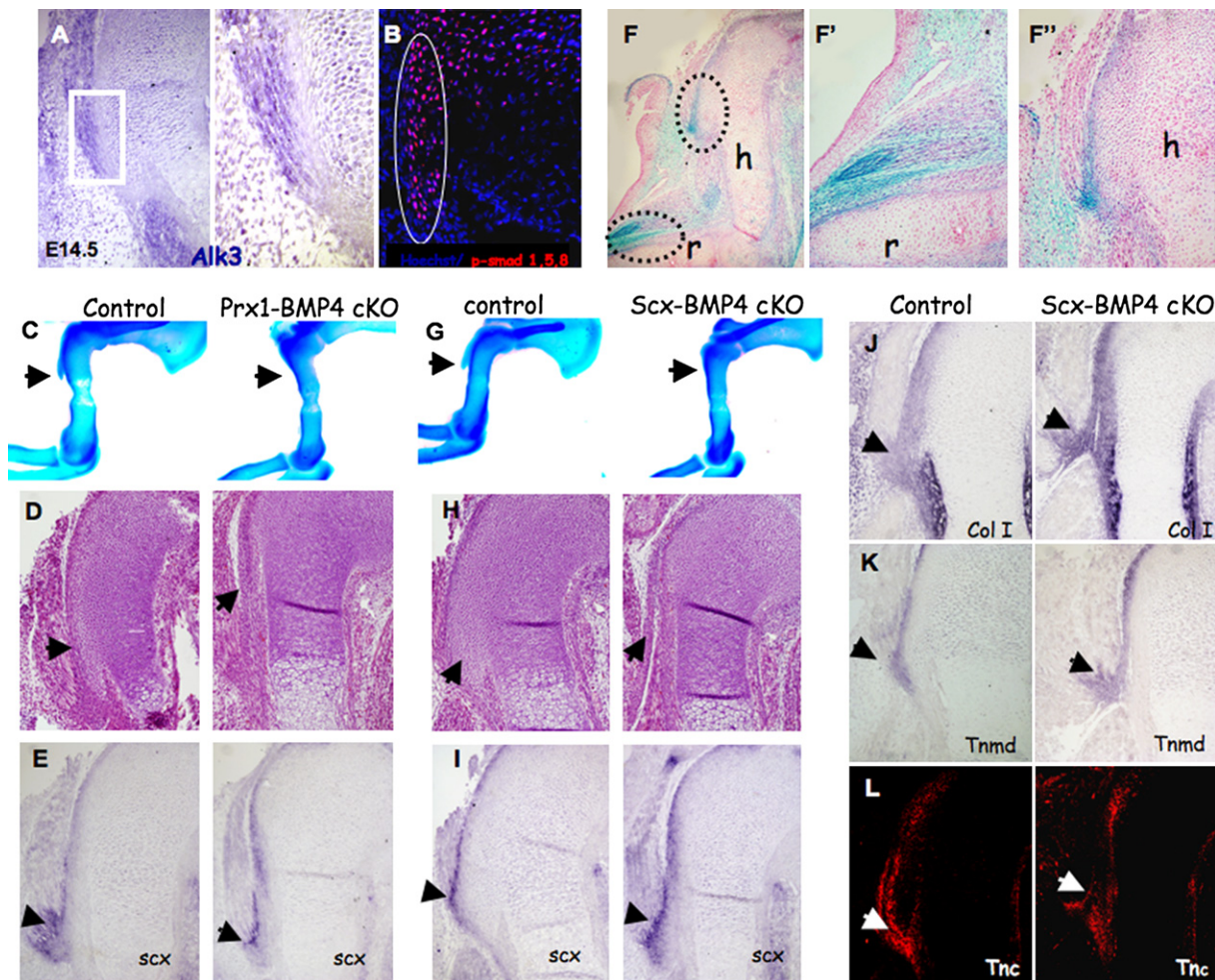
steady-state level of *Bmp4* mRNA was a consequence of increased transcription, we transiently cotransfected C3H10T1/2 and HeLa cell lines with a construct that contained a 0.9 kb of *Bmp4* promoter region fused to luciferase cDNA (pGL3 BMP4 full) and Scx-expressing vector. These experiments revealed approximately 3-fold induction of luciferase activity relative to the control vector (Figure 4G; for C3H10T1/2 cells, data not shown).

Next, we searched the mouse *Bmp4* promoter for SCX consensus binding sites (also referred to as E-box). We identified two putative binding sites in positions  $-242$  (CACGTG) and  $-230$  (CAGGTG) upstream to the transcription initiation site (Figure 4H); these consensus sequences were previously shown to bind scleraxis (Lejard et al., 2007; Liu et al., 1997). In order to examine whether these two E-boxes were necessary for SCX induction of *Bmp4* expression, we made two constructs: one with mutated E-boxes (pGL3 B4mut: CACGTG–CACAAA, CAGGTG–CAGAAA) and another that contained a region down-

stream of the E-Boxes (pGL3 del1). We compared the ability of SCX to induce luciferase activity in the mutated promoter and in the intact promoter. As can be seen in Figure 4H, as well as indicating a deletion of the *Bmp4* promoter, the two mutations of the E-boxes blocked the ability of SCX to induce luciferase activity.

In order to demonstrate a direct binding of scleraxis protein to the *Bmp4* promoter, we performed a chromatin immunoprecipitation (ChIP) experiment. Chromatin was prepared from C3H10T1/2 cells lysate stably expressing Scx tagged with Xpress epitope. The lysate was incubated with either an anti-Xpress-tag antibody or anti-GFP antibody (as control). qRT-PCR analysis using specific primers to the E-boxes region of *Bmp4* promoter revealed binding of SCX to the indicated promoter region (Figure 4I).

To further validate the specificity of the two identified E-box sequences for SCX binding, we utilized a plasmid IP experiment. To that end, HeLa cells where cotransfected with Scx-expressing

**Figure 5. BMP4 Mediates DT Initiation**

(A) In situ hybridization of DT sagittal sections from E14.5 WT mice using anti-sense complementary RNA probes for *Alk3*.  
 (A') Enlargement of the boxed area in (A) highlights the border between DT and tendon cells.  
 (B) Sagittal sections through the humerus of WT E14.5 embryo counterstained with anti-P-Smad 1/5/8 antibody (circle indicates DT area).  
 (C and G) Skeleton preparation and (D and H) histological sagittal sections through the humeri of E14.5 *Prx1-Bmp4* and *Scx-Bmp4* mutants lack the DT.  
 (E and I) In situ hybridization of DT sagittal sections from E14.5 mice, using anti-sense complementary RNA probes for *Scx*.  
 (F) Section of whole-mount  $\beta$ -gal staining of E14.5 *Scx-Cre*, R26R-*lacZ* limbs demonstrates  $\beta$ -galactosidase activity in the tendons. Enlargements of the boxed areas highlight the insertion of tendons to (F') the radius bone and to (F'') the DT.  
 (J-L) Examination of tendon differentiation in *Scx-Bmp4* mutants.  
 (J and K) In situ hybridization of humerus sagittal sections from E14.5 mice, using anti-sense complementary RNA probes for *Col1a1* and *Tnmd* mRNA.  
 (L) Sagittal sections from E14.5 control and *Scx-Bmp4* mutants stained with anti-tenascin C (TNC) antibody.

plasmid together with either the intact *Bmp4* promoter (pGL3 B4 full) or the *Bmp4* promoter with the mutated E-boxes (pGL3 B4mut). As can be seen in Figure 4J, qRT-PCR analysis revealed that the mutations in the E-boxes completely ablated the binding of SCX to the *Bmp4* promoter. Therefore, we conclude that scleraxis binds the *Bmp4* promoter and regulates its transcription.

#### Bmp4 Expression in Tendons Regulates DT Initiation

To establish that BMP4 mediates signaling from tendons to cartilage in the regulation of bone ridge initiation, we wanted to demonstrate that BMP signaling was activated in the initiating DT and was required for its formation. To detect an activation

of BMP signaling in chondrocytes of the forming DT, we examined the expression of *Alk3*, a type IA receptor for BMP4 (*BmprlA*) (Yamaji et al., 1994). In E14.5 control mice, *Alk3* was expressed within muscles and cartilage, but not in tendons (Figure 5A). Next, we directly tested the activation of the BMP pathway by examining the activation of Smad proteins, the downstream mediators of the BMP signaling cascade (Shi and Massague, 2003), using a specific antibody that detects the phosphorylated form of Smad 1, 5, and 8 (P-Smad). P-Smad 1/5/8 staining in E14.5 WT forelimb was observed in DT chondrocytes (Figure 5B). Taken together, these results support the notion that SCX-dependent expression of *Bmp4* in tendons activates BMP signaling in tuberosity-forming chondrocytes.

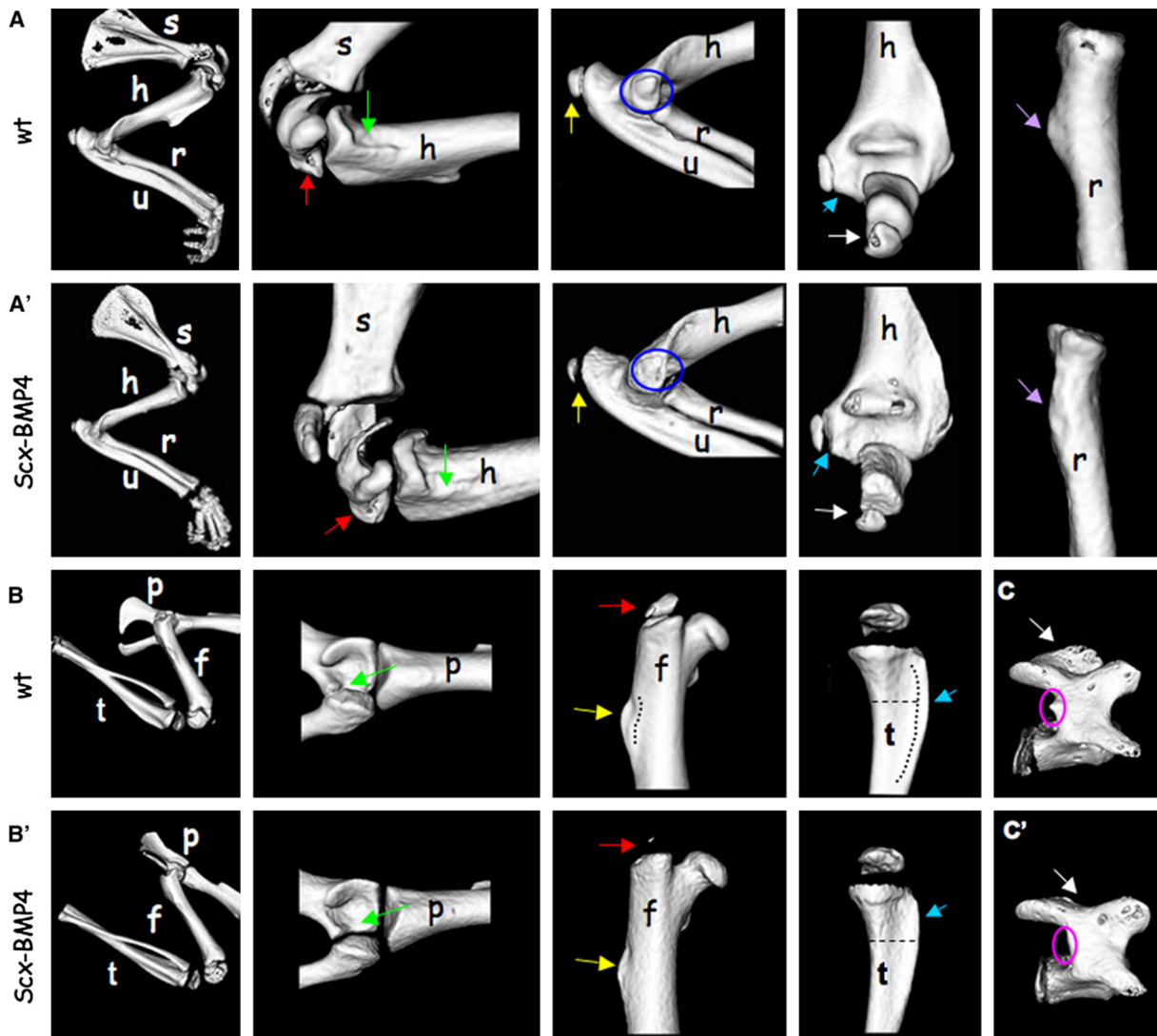


**Figure 6. The Loss of *Bmp4* in Tendons Has a Wide Effect on Bone Ridge Development throughout the Skeleton**

Micro-CT analysis of 14 day old WT and *Scx-Bmp4* mice showing bone ridges located on the (A and A') forelimbs, (B and B') hindlimbs, and (C and C') vertebrae. (A) Green arrows indicate the ridge distal to the minor tubercle on the medial aspect of the humerus. Red arrows indicate the greater tubercle of the humerus. Yellow arrows indicate the olecranon of the ulna. Blue circles indicate the medial epicondyle of the humerus. Blue arrows indicate lateral epicondyle of the humerus. White arrows indicate the olecranon of the ulna. Purple arrows indicate the radial tuberosity, located on the radius. (B) Green arrows indicate the lunate surface of the acetabulum, located on the pelvis. Red arrows indicate the greater trochanter of the femur. Yellow arrows indicate the third trochanter of the femur. Blue arrows indicate the tibial crest. (C) Pink circles indicate the accessory process on the lamina of the vertebra. White arrows indicate the spinous process of the vertebra. Abbreviations: s, scapula; h, humerus; r, radius; u, ulna; p, pelvis; f, femur; t, tibia.

To establish that BMP signaling to chondrocytes was imperative for DT initiation, we blocked the expression of *Bmp4* in limb mesenchyme using the *Prx1-Cre* as a deleter (*Prx1-Bmp4*). Examination of skeletal preparation and histological sections of E14.5 *Prx1-Bmp4* limbs revealed the lack of DT initiation (Figures 5C and 5D). To further demonstrate that this phenotype was specifically related to *Bmp4* abolishment in tendon cells, we blocked the expression of *Bmp4* in *Scx*-expressing cells using the *Scx-Cre* as a deleter (*Scx-Bmp4*; the *Scx-Cre* mice will be reported elsewhere). To evaluate the effectiveness and specificity of *Scx-Cre* as a deleter in tendon cells, we crossed the *Scx-Cre*

mice with R26R-*lacZ* reporter mice (Soriano, 1999). Examination of *Scx-Cre*, R26R-*lacZ* heterozygous embryos at E14.5 revealed *lacZ* expression in the forming tendons (Figure 5F).

Next, we examined skeletal preparations and histological sections of limbs from E14.5 *Scx-Bmp4* embryos and detected no DT initiation (Figures 5G and 5H). To exclude the possibility that tuberosity loss resulted from the lack of tendons in these mutants' limbs, or that *Bmp4* expression was necessary for the expression of *Scx* in these limbs, we examined histological sections and the expression of *Scx* in limbs of *Prx1-Bmp4* and *Scx-Bmp4* embryos. *Scx* expression was not affected in the

mutated limbs (Figures 5E and 5I) and tendons did form in their presumed attachment site to the humerus (see Figure S3B and S3C available online); moreover, these tendons apparently attached directly to the perichondrium instead of to the DT, as in the control limbs. Further analysis of tendon integrity was conducted on the *Scx-Bmp4* embryos by examining the expression of *Scx*, collagen type I alpha 1 (*Col1a1*), tenomodulin (*Tnmd*), and tenascin C (*Tnc*), markers of tendon differentiation. The expression of *Scx*, *Col1a1*, *Tnmd*, and *Tnc* in mutants' tendons (Figures 5J–5L) indicated normal differentiation.

Finally, to evaluate the contribution of *Bmp4* expression in tendons to bone ridge formation throughout the skeleton, we examined the development of a wide variety of bone ridges in 2-week-old *Scx-Bmp4* mice by micro-CT scanning. As can be seen in Figure 6, the loss of *Bmp4* in tendons led to aberrant formation of numerous ridges in the axial and appendicular skeleton; however, not all the ridges were affected.

These results strongly support our hypothesis that SCX regulation of *Bmp4* expression in tendons regulates bone ridge initiation. Moreover, these results implicate BMP4 as a key molecule in the mechanism that mediates signaling from tendon cells to chondrocytes at their attachment site.

## DISCUSSION

Bone ridges are critical for the ability of the skeleton to cope with the mechanical load applied by the musculature. In this study, we show that tendon attachment to the skeleton regulates bone ridge formation and identify SCX regulation of *Bmp4* as the underlying molecular mechanism. Moreover, we describe the contribution of muscular activity to the regulation of the bone ridge size. This study examines the development of the skeleton as part of the musculoskeletal system, demonstrating the centrality of cartilage-tendon interaction for secondary patterning of the skeleton.

### DT as a Miniature Growth Plate

Bone ridges are poorly studied. Notwithstanding, several studies have been performed on postnatal skeletons, focusing on the connective tissue interface between skeleton and tendons, which is classified as either fibrous or fibrocartilaginous according to the tissue that occupies the attachment site (Benjamin et al., 2002, 2006).

We show that the DT is formed through endochondral ossification (Figure 1). Hence, this lateral outgrowth from the humerus does not represent a new cellular mechanism for the generation of skeletal tissue, but rather a deployment of the cellular and molecular cascade of endochondral bone formation along a secondary axis. Considering the large variability of bone ridge morphology, it is yet to be determined whether they all develop by the same process.

In contrast to primary growth plates, the formation of the growth plate of the DT is dependent on tendons and muscles (Figures 2A–2D, and 3C; Figures S1A–S1C). This difference in the mode of regulation suggests that during development, the skeleton is regulated by at least two different programs. The first is the intrinsic genetic program that largely regulates the initial steps in bone formation. Later on, when the skeleton begins to interact with tendons and muscles, signals from these tissues

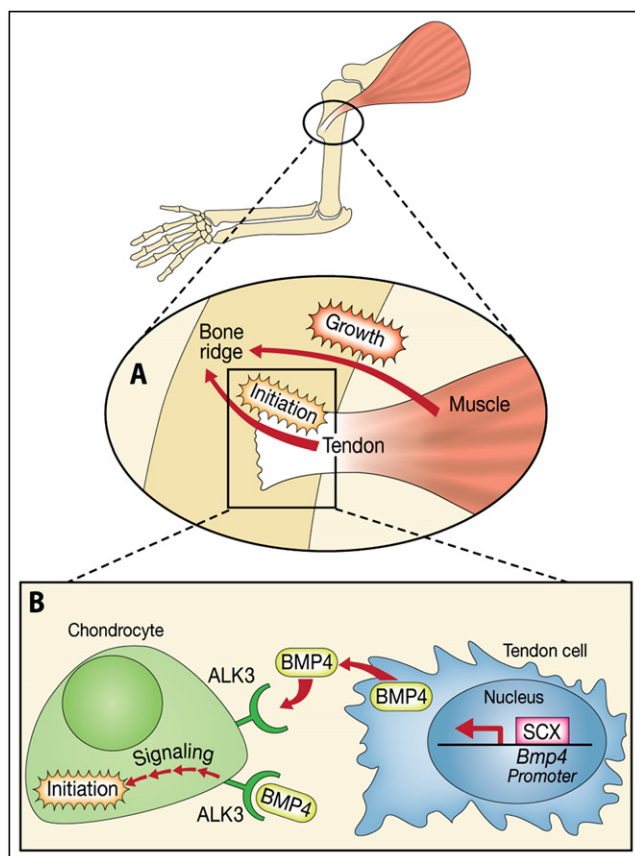


**Figure 7. Our Model for Bone Ridge Formation by a Biphasic Process**

A scheme of the forelimb skeleton that illustrates the involvement of tendons and muscles in bone ridge formation.

(A) Magnification of the circled area at the scheme above. We suggest a model for the contribution of both tendons and muscles to bone ridge formation in a biphasic process, as tendons regulate tuberosity initiation and muscles control its subsequent growth. While we have begun to reveal the molecular mechanism that underlies tendon regulation of bone ridge initiation, the mechanism whereby muscle contraction regulates bone ridge growth remains to be uncovered.

(B) Magnification of the squared area in (A). Focusing on tendon-cartilage interaction in the initiation phase, we identify the bHLH transcription factor SCX as a regulator of *Bmp4* expression in tendon cells. Next, upon binding of BMP4 to its receptor ALK3 in chondrocytes, a signaling cascade is activated leading, eventually, to the initiation of a bone ridge.

contribute to its secondary patterning. We speculate that this extrinsic regulation ensures the proper assembly of the musculoskeletal system and its adaptation to the changing requirements of the organism.

Our observation that similarly to long bones, the DT forms by a growth plate highlights the evolutionary advantage of this cellular mechanism in bone formation. Yet, the difference in the mode of regulation between these distinct growth plates illustrates its modularity.

### The Molecular Mechanism Underlying Tendon Regulation of DT Formation

The initiation of the DT at E13.5 (Figures 1D and 1E) is synchronized with the differentiation of tendons and muscles at their

attachment site to the skeleton (Ontell et al., 1993; Murchison et al., 2007). This concurrence allows for a regulatory crosstalk among the various musculoskeletal tissues. Indeed, using the *Prx1-Tgf-βRII* mutant as a model for “tendon-less” mice (Pryce et al., 2009), we demonstrate that the initiation of bone ridges such as the DT and the third trochanter of the femur does not occur in the absence of tendons (Figures 3A–3C; Figure S1C). This clearly implies the centrality of tendons in bone ridge development.

In *Prx1-Tgf-βRII* embryos, TGFβ signaling was disrupted throughout the limb mesenchyme. The failure in DT growth in these mutants could also be attributed to the disruption of TGFβ signaling in chondrogenic tissues. However, the DT was not affected when *Tgf-βRII* expression was targeted in chondrocytes, using the *Col2a1-Cre* deleter (Baffi et al., 2004).

The concept that a crosstalk between a tendon and the tissue to which it attaches is necessary for the development of the musculoskeletal system was previously demonstrated in *Drosophila* (Volk, 1999). In the *Drosophila* embryo, tendon cells direct myotube migration and final patterning, while muscles are essential for the maintenance of the fate of tendon cells. Another example for the active role that tendons play during the assembly of the musculoskeletal system was found in incidences of human congenital defects, in which tendons were attached to structures other than their normal “targets” (Graham et al., 1982). These observations suggest that tendons may be actively involved in determining their attachment site.

Our genetic and molecular data clearly demonstrate that *Bmp4* expression in tendons is necessary for the initiation of bone ridges such as the DT (Figures 5C and 5G). Consistent with our findings, the abrogation of *Bmpr1a* expression in limb mesenchyme led to the formation of a humerus devoid of a tuberosity (Ovchinnikov et al., 2006). Our finding that some ridges and tuberosities were formed in mice in which *Bmp4* expression was blocked in tendon cells suggests that other signaling molecules may play a role in this process. Support for this supposition comes from a previous study in mice with a dominant-negative *Bmp5* mutation that suggested the involvement of BMP signaling in bone ridge response to mechanical stimulation (Ho et al., 2008). Given that BMP4 regulates DT initiation, it is possible that various BMPs are involved in the regulation of bone ridge development at different stages.

Relatively little is known about the molecular players that mediate the regulatory interactions among the tissues of the musculoskeletal system during its assembly (Tozer and Duprez, 2005). Previous studies have shown in somites that FGFs from the myotome induce adjacent sclerotomal cells to become tendon cells (Brent et al., 2003; Brent and Tabin, 2004). Other molecules that emanate from muscles and cartilage to regulate tendon formation are the TGFβs (Pryce et al., 2009). Complementing these studies, we show that SCX regulation of *Bmp4* in tendons serves as the reciprocal signal by which tendons regulate cartilage at the attachment site.

Another open question raised by this study regards the mechanism that specifies a field of cells in the developing humerus, which upon receiving the BMP4 signal gives rise to the formation of the DT. Since the expression of *Bmp1A* was not restricted to tuberosity-forming chondrocytes and *Bmp4* expression was restricted to tendon insertion sites, it is possible that the diffusion

capability of BMP4 is the factor that determines and restricts this field. Another hypothesis is the existence of bone ridge progenitor cells that respond to the signal emanating from the tendons. To validate this hypothesis, it is necessary to identify molecular markers associated with these progenitor cells, as well as the signal that activates them.

### The Assembly of the Musculoskeletal System Dictates a Biphasic Process for DT Formation

The influence of stress and strain on the bone was well established in the early days of bone research (Koch, 1917; Wolff, 1892; Roux, 1881). Studies by Pottorf (1916) and Howell (1917) clearly demonstrated that the effect of mechanical load created by muscle contraction was much more dramatic than the effect of weight pressure. A role for muscle-induced mechanical load in the formation of bone ridges was first suggested following bone transplantation studies (Hamburger, 1938, 1939, 1940). In these experiments, the humerus was transplanted to the umbilical cord leading to a reduction in the size of the DT, thus indicating the need for a proper musculoskeletal junction to ensure a normal bone ridge development. Studies on immobilized chick embryos (Hall and Herring, 1990; Hosseini and Hogg, 1991) and mice that lacked either skeletal muscles or muscle contractility further indicated the contribution of muscle contraction to tuberosity formation (Pai, 1965a; Rot-Nikcevic et al., 2006; Tremblay et al., 1998). Interestingly, human patients with a contracture of the deltoid muscle exhibit an enlargement of the DT (Ogawa et al., 1999).

Based on our developmental analysis, we support a role for the musculature in bone ridge formation. However, we demonstrate that the formation of the DT and other bone ridges, such as the third trochanter, is initiated in the absence of contracting muscles (Figures 2C and 2D; Figure S1A). Furthermore, chondrocytes in the DT of these mutants even differentiate to hypertrophy (Figures 2E–2I). It is, in fact, the subsequent growth phase, which unfolds via chondrocyte proliferation, that depends on muscle contraction, as in its absence the DT ceased to develop and was ultimately engulfed by the growing humerus (Figure S2).

These observations led us to conclude that bone ridges are formed through a two-phase process. During the initiation phase, tendons are sufficient and muscles are dispensable, whereas tuberosity growth during the subsequent phase is muscle-dependent. The reason for the selection of such a biphasic developmental process may lie in the need of the attachment site to supply sufficient initial anchoring capabilities. Thus, the regulation of bone ridge initiation is predetermined. Once a substantial size is achieved, the regulation can be then coupled to muscular activity, allowing for a tight, dynamic coordination between physical strain on one hand, and anchoring and force dissipation capabilities on the other.

The existence of tendon cells at the attachment site, without respect to the formation of a functioning musculature (Figures 3H and 3J), was also reported in *Myf5*<sup>−/−</sup>; *MyoD*<sup>−/−</sup> mice (Brent et al., 2005) and in chick embryos (Kardon, 1998). However, later in development, tendon formation requires the presence of muscles (Bonnin et al., 2005; Brent et al., 2005; Edom-Vovard et al., 2002; Kardon, 1998; Kieny and Chevallier, 1979; Schweitzer et al., 2001). In view of these observations, the extent of

tendon involvement in tuberosity growth during the second phase remains an open question. It is yet to be determined whether tendon cells, in response to muscle contraction, produce a signal that induces growth in the tuberosity cells, or whether tendinous tissue acts passively by transmitting to the tuberosity forming cells the force applied by the musculature, which regulates their proliferation.

This study describes the interaction that occurs during embryogenesis among the three components of the musculoskeletal system at their intersection point, the bone ridge. We reveal the regulatory role of muscles and tendons in cartilaginous bone ridge formation and identify SCX regulation of *Bmp4* as the molecular mechanism that underlies the induction of tuberosity development by tendons (Figure 7). These findings provide a new perspective on the regulation of skeletogenesis in the context of the musculoskeletal system and shed light on the mechanism that underlies the assembly of this system.

## EXPERIMENTAL PROCEDURES

### Animals

Heterozygous *Sp<sup>d</sup>* mice (Dickie, 1964) and *Scx<sup>-/-</sup>* mice (Murchison et al., 2007) have been previously described. Mice heterozygous for the mutation muscular dysgenesis (*mdg*) (Pai, 1965a) were kindly provided by G. Kern, Innsbruck, Austria. The generation of *floxed-Prx1-Tgf-βRII* (Chytil et al., 2002), *Prx1-Cre* (Logan et al., 2002), and *Bmp4* conditional allele (Liu et al., 2004; Selever et al., 2004) have been described previously. The generation of *Scx-Cre* transgenic mice will be described elsewhere by R. Schweitzer and R.L. Johnson. To create *Sp<sup>d</sup>*, *mdg*, and *Scx<sup>-/-</sup>* mutant mice, animals heterozygous for the mutation were crossed; as a control we used heterozygous *Sp<sup>d</sup>*, *mdg*, and *Scx* embryos.

To create *Prx1-Tgf-βRII* and *Prx1-Bmp4* mutant mice, *floxed-Tgf-βRII* and *floxed-Bmp4* mice were mated to *Prx1-Tgf-βRII* and *Prx1-Bmp4*. As a control, we used embryos heterozygous for *floxed-Tgf-βRII* or *floxed-Bmp4* and *Prx1-Cre* alleles. To create *Scx-Bmp4* conditional mutant mice, *floxed-Bmp4* mice were mated to *Scx-Bmp4* mice; as a control, we used embryos heterozygous for *floxed-Bmp4* and *Scx-Cre* alleles.

In all timed pregnancies, plug date was defined as E0.5. For harvesting of embryos, timed-pregnant females were sacrificed by CO<sub>2</sub> intoxication. The gravid uterus was dissected out and suspended in a bath of cold phosphate-buffered saline (PBS), and the embryos were harvested after amniocentesis and removal of the placenta. Tail genomic DNA was used for genotyping.

### Skeletal Preparations

Cartilage and bones in whole mouse embryos were visualized after staining with Alcian blue and Alizarin red S (Sigma) and clarification of soft tissue with KOH (McLeod, 1980).

### Micro-CT Analysis

Three-dimensional images were obtained from the left hindlimb, forelimb, and lumbar vertebrae of *Scx-Bmp4* mice using microcomputed tomography (GE Healthcare, London, Ontario, Canada). Scans were taken at 16-micron isotropic resolution and images were reconstructed and thresholded to distinguish bone voxels with MicroView software version 5.2.2 (GE Healthcare). One threshold was chosen for all specimens.

### Histological Analysis and In Situ Hybridization

For histology and in situ hybridization, embryos were sacrificed at various ages, dissected, and fixed in 4% paraformaldehyde (PFA)/PBS at 4°C overnight. After fixation, tissues were dehydrated to 100% ethanol and embedded in paraffin. The embedded tissues were cut to generate 7 μm thick sections and mounted onto slides.

Section in situ hybridizations were performed as described previously (Martaugh et al., 1999; Riddle et al., 1993). All probes are available by request.

Hematoxylin and eosin (H&E) staining was performed following standard protocols. Double fluorescent in situ hybridizations on paraffin sections were performed using biotin- and DIG-labeled probes. After hybridization slides were washed, quenched, and blocked. Probes were detected by incubation with streptavidine-HRP (Perkin Elmer, diluted 1 in 1500) and anti-DIG-HRP (Roche, dilute 1 in 50), followed by Cy3- or Cy2-tetramide labeled fluorescent dyes (according to the instructions of the TSA Plus Fluorescent Systems Kit, Perkin Elmer).

### BrdU Assay

Pregnant mice were injected intraperitoneally with 100 mg/kg body weight of BrdU labeling reagent (Sigma) and sacrificed 2 hr later. Embryo tissues were fixed in 4% PFA at 4°C overnight, processed, and embedded in paraffin. Sections of the limb were cut at 7 μm, dewaxed, and rehydrated. Antigen retrieval was performed by microwaving the sections in 0.01 M sodium citrate buffer (pH 6.0). Sections were then washed with 1% bovine serum albumin/PBS-Triton wash buffer (PBS +0.5% Triton). In order to block nonspecific binding of immunoglobulin, sections were incubated with 1% bovine serum albumin + 5% goat serum for 60 min at room temperature. After blockage, sections were incubated with the primary antibody G3G4 anti-BrdU (1:100; DSHB, The University of Iowa) overnight at 4°C. Then, sections were washed in PBS and incubated with the secondary fluorescent antibody, Alexa 568 (1:100; Invitrogen). To quantify the rate of cell proliferation, serial images of the same humerus were collected and BrdU-positive chondrocytes (red) and -negative chondrocytes (gray) in the DT tip region were counted. At least three sections were counted for each of four control and *mdg* mutant littermate embryos at E14.5 and E16.5. Statistical significance was determined by Student's t test.

### Whole-Mount β-Galactosidase Staining

Embryos were fixed for 1 hr in 4% PFA at 4°C, washed three times in rinse buffer containing 0.01% deoxycholate, 0.02% NP-40, 2 mM MgCl<sub>2</sub>, and 5 mM EGTA at room temperature, and stained for 3 hr at 37°C in rinse buffer supplemented with 1 mg/ml X-gal, 5 mM K3 Fe(CN)<sub>6</sub>, and 5 mM K4 Fe(CN)<sub>6</sub>. For histological examination, stained whole-mount limbs were fixed in 4% PFA overnight, dehydrated, embedded in paraffin, and used to generate 7 mm thick sections, which were collected on Fisherbrand Superfrost Plus slides, dehydrated, and cleared in xylene.

### Immunofluorescence

For immunofluorescence, embryo limbs were embedded in OCT (Tissue-Tek®) after 2–6 hr fixation in 4% PFA and 10 μm cryostat sections were made. Cryosections were postfixed for 30 min in 4% PFA and permeabilized with 0.2% Triton/PBS. In order to block nonspecific binding of immunoglobulin, sections were incubated with 7% goat serum. Following blockage, cryosections were incubated overnight at 4°C with primary antibodies: anti-collagen II (1:100; DSHB, University of Iowa), anti-tenascin C (1:100; Harold Erickson, Duke University). Then, sections were washed in PBS and incubated with secondary fluorescent antibodies Cy3 (1:100; Jackson Laboratories). The signal of the transgenic tendon reporter *ScxGFP* was captured directly from alternating cryosections. Hoechst was used for counterstaining.

### Vectors

Express epitope-tagged *Scx* cDNA (a kind gift from J. Rossert) was cloned into pEF-IRES-puro vector. A 0.8 kb fragment of *Bmp4* promoter (a kind gift from C.G. Kim) (Kang et al., 2004) was cloned into pGL3 vector upstream of luciferase ORF. Mutations of E-boxes in positions –242 and –230 in the *Bmp4* promoter were produced by PCR using the following primers: TGCTTCTAG TACCTCTTGCACAAAGTCCCCAGAAAAGCCCGGCTGCTCCCGAG and its anti-sense (mutated regions underlined).

### Tissue Culture, Transfections, Luciferase Assay, and Stable Lines Preparation

C3H10T1/2 cells (a kind gift from D. Zipori) were kept in culture according to ATCC recommendations. For *Bmp4* promoter experiments, 1 μg of pGL3 *Bmp4* was cotransfected in 6-well plates with 2 μg of pEF-Scx-IRES-puro or with empty vector to HeLa or C3H10T1/2 cells using JetPei reagent. Each well was also cotransfected with 200 ng of renilla-expressing plasmid.

Luciferase assay was performed 48 hr posttransfection and the results were normalized to Renilla activity. For transient Scx overexpression in C3H10T1/2 cells, they were transfected using Lipofectamine 2000 reagent (Invitrogen) according to the manufacturer's instructions and cells were harvested after 48 hr. In order to obtain a cell line stably overexpressing Scx, C3H10T1/2 cells were transfected with pEF-Scx-IRES-puro construct or with empty vector and selected with 3  $\mu$ g/ml of puromycin (Sigma). The presence of SCX in the resulting lines was verified by western blot with anti-express epitope antibody (Invitrogen). All experiments described above were performed at least three times.

#### Quantitative RT-PCR (qRT-PCR)

In each experiment, RNA was purified using RNAeasy kit (QIAGEN). cDNA was synthesized from 1  $\mu$ g of RNA with SuperScript II First-Strand kit (Invitrogen).

qRT-PCR was performed using SYBR Green (Roche). Values were calculated with the second derivative method and normalized to actin expression. For PCR, the following primers were used:

*Bmp4*: sense, GTGACACGGTGGAAACTTCGAT, anti-sense, CACCTCAATGGCCAGCCATAAT;

*Scx*: sense, CAGCCCAAACAGATCTGCACCTT, anti-sense, TTGGAATCGCCGTCTTCTGTCA.

#### Chromatin Immunoprecipitation

Chromatin preparation and ChIP were performed as described previously (Amarilio et al., 2007). For IP, 1  $\mu$ g of either mouse anti-Xpress antibody (Invitrogen) or anti-GFP antibody (Abcam) was added to sonicated chromatin corresponding to 1 million cells. Purified DNA from immunoprecipitates, as well as of the input material, was analyzed by qRT-PCR using primers specific to the region of the E-boxes: B4 sense, AAGCCAGACTCCATGGGTATTT; B4 anti-sense, GGAAGATTGCACAGCTCCCCA. As a control we used primers specific to the region of pGL3 plasmid 2.5 kb away from the cloned promoter: pGL3 sense, CAGGGGATAACGCAGGAAAGAAC; pGL3 anti-sense, AAAGCGGCACAGGTATCCGGTAA. Results were normalized and presented as percentage of input DNA.

#### Formaldehyde Crosslinked Immunoprecipitation

For immunoprecipitation of exogenous mouse *Bmp4* promoter, 70% confluent HeLa cells in 14 cm dishes were cotransfected with pEF-Scx-IRES-Puro and pGL3-*Bmp4* WT promoter or promoter with mutated E-boxes. For analysis of the endogenous promoter, C3H10T1/2 cells stably transfected with pEF-Xpress-*mScx*-IRES-Puro or with empty vector were used. In all the experiments cells were crosslinked with 1% formaldehyde for 15 min and trypsinized.

#### SUPPLEMENTAL DATA

Supplemental Data include three figures and can be found with this article online at [http://www.cell.com/developmental-cell/supplemental/S1534-5807\(09\)00432-8](http://www.cell.com/developmental-cell/supplemental/S1534-5807(09)00432-8).

#### ACKNOWLEDGMENTS

We are grateful to G. Kern, Innsbruck, Austria, for the *mdg* mice. Plasmids and cell lines were kindly provided by J. Rossert, C.G. Kim, and D. Zipori. The authors wish to thank T. Volk, B. Shilo, and R. Shachar for their helpful reviews of the manuscript and to N. Konstantin for expert editorial assistance. We thank S. Kerief and D. Loeliger for expert technical support. Special thanks to all members of the Zelzer laboratory for advice and suggestions. We thank A. Florentin and the Graphic Design Department of Weizmann Institute of Science for their help with designing the graphic model. This work was supported by grants from Israel Science Foundation grant 499/05, Minerva grant M941, The Leo and Julia Forchheimer Center for Molecular Genetics, The Stanley Chais New Scientist Fund, The Kirk Center for Childhood Cancer and Immunological Disorders, The David and Fela Shapell Family Center for Genetic Disorders Research, The Clore Center for Biological Physics, Benoziyo Institute, NIH grant PO1 DK56246 (to C.J.T.), NICHD grant F32HD057701 (to J.L.G.), and NIAMS grant R01 AR055640 (to R.S.). E.Z. is the incumbent of the Martha S. Sagon Career Development Chair.

Received: February 12, 2009

Revised: September 17, 2009

Accepted: October 22, 2009

Published: December 14, 2009

#### REFERENCES

Amarilio, R., Viukov, S.V., Sharir, A., Eshkar-Oren, I., Johnson, R.S., and Zelzer, E. (2007). HIF1 $\alpha$  regulation of Sox9 is necessary to maintain differentiation of hypoxic prechondrogenic cells during early skeletogenesis. *Development* 134, 3917–3928.

Baffi, M.O., Slattery, E., Sohn, P., Moses, H.L., Chyttil, A., and Serra, R. (2004). Conditional deletion of the TGF- $\beta$  type II receptor in Col2a expressing cells results in defects in the axial skeleton without alterations in chondrocyte differentiation or embryonic development of long bones. *Dev. Biol.* 276, 124–142.

Benjamin, M., Kumai, T., Milz, S., Boszczyk, B.M., Boszczyk, A.A., and Ralphs, J.R. (2002). The skeletal attachment of tendons–tendon “enthesis”. *Comp. Biochem. Physiol. A Mol. Integr. Physiol.* 133, 931–945.

Benjamin, M., Toumi, H., Ralphs, J.R., Bydder, G., Best, T.M., and Milz, S. (2006). Where tendons and ligaments meet bone: attachment sites (“enthesis”) in relation to exercise and/or mechanical load. *J. Anat.* 208, 471–490.

Biewener, A.A., Fazzalari, N.L., Konieczynski, D.D., and Baudinette, R.V. (1996). Adaptive changes in trabecular architecture in relation to functional strain patterns and disuse. *Bone* 19, 1–8.

Bonnin, M.A., Laclef, C., Blaise, R., Eloy-Trinquet, S., Relaix, F., Maire, P., and Duprez, D. (2005). Six1 is not involved in limb tendon development, but is expressed in limb connective tissue under Shh regulation. *Mech. Dev.* 122, 573–585.

Brent, A.E., and Tabin, C.J. (2004). FGF acts directly on the somitic tendon progenitors through the Ets transcription factors Pea3 and Erm to regulate scleraxis expression. *Development* 131, 3885–3896.

Brent, A.E., Schweitzer, R., and Tabin, C.J. (2003). A somitic compartment of tendon progenitors. *Cell* 113, 235–248.

Brent, A.E., Braun, T., and Tabin, C.J. (2005). Genetic analysis of interactions between the somitic muscle, cartilage and tendon cell lineages during mouse development. *Development* 132, 515–528.

Chyttil, A., Magnuson, M.A., Wright, C.V., and Moses, H.L. (2002). Conditional inactivation of the TGF- $\beta$  type II receptor using Cre:Lox. *Genesis* 32, 73–75.

Cserjesi, P., Brown, D., Ligon, K.L., Lyons, G.E., Copeland, N.G., Gilbert, D.J., Jenkins, N.A., and Olson, E.N. (1995). Scleraxis: a basic helix-loop-helix protein that prefigures skeletal formation during mouse embryogenesis. *Development* 121, 1099–1110.

Dickie, M.M. (1964). New Splotch alleles in the mouse. *J. Hered.* 55, 97–101.

Edom-Vovard, F., Schuler, B., Bonnin, M.A., Teillet, M.A., and Duprez, D. (2002). Fgf4 positively regulates scleraxis and tenascin expression in chick limb tendons. *Dev. Biol.* 247, 351–366.

Franz, T., Kothary, R., Surani, M.A., Halata, Z., and Grim, M. (1993). The Splotch mutation interferes with muscle development in the limbs. *Anat. Embryol. (Berl.)* 187, 153–160.

Graham, J.M., Jr., Stephens, T.D., Siebert, J.R., and Smith, D.W. (1982). Determinants in the morphogenesis of muscle tendon insertions. *J. Pediatr.* 101, 825–831.

Hall, B.K., and Herring, S.W. (1990). Paralysis and growth of the musculoskeletal system in the embryonic chick. *J. Morphol.* 206, 45–56.

Hamburger, V. (1938). Morphogenetic and axial self-differentiation of transplanted limb primordia. *J. Exp. Zool.* 77, 379–399.

Hamburger, V. (1939). The development and innervation of transplanted limb primordia of chick embryos. *J. Exp. Zool.* 80, 347–389.

Hamburger, V. (1940). The primary development of the skeleton in nerveless and poorly innervated limb transplants of chick embryos. *Physiol. Zool.* 13, 367–384.

Ho, A.M., Marker, P.C., Peng, H., Quintero, A.J., Kingsley, D.M., and Huard, J. (2008). Dominant negative Bmp5 mutation reveals key role of BMPs in skeletal response to mechanical stimulation. *BMC Dev. Biol.* 8, 35.

Hosseini, A., and Hogg, D.A. (1991). The effects of paralysis on skeletal development in the chick embryo. I. General effects. *J. Anat.* 177, 159–168.

Howell, J.A. (1917). An experimental study of the effect of stress and strain on bone development. *Anat. Rec.* 13, 223–252.

Isaac, A., Rodriguez-Esteban, C., Ryan, A., Altabef, M., Tsukui, T., Patel, K., Tickle, C., and Izpisua-Belmonte, J.C. (1998). Tbx genes and limb identity in chick embryo development. *Development* 125, 1867–1875.

Kang, H.C., Chae, J.H., Kim, B.S., Han, S.Y., Kim, S.H., Auh, C.K., Yang, S.I., and Kim, C.G. (2004). Transcription factor CP2 is involved in activating mBMP4 in mouse mesenchymal stem cells. *Mol. Cells* 17, 454–461.

Kardon, G. (1998). Muscle and tendon morphogenesis in the avian hind limb. *Development* 125, 4019–4032.

Karsenty, G., and Wagner, E.F. (2002). Reaching a genetic and molecular understanding of skeletal development. *Dev. Cell* 2, 389–406.

Kieny, M., and Chevallier, A. (1979). Autonomy of tendon development in the embryonic chick wing. *J. Embryol. Exp. Morphol.* 49, 153–165.

Koch, J.C. (1917). The laws of bone architecture. *Am. J. Anat.* 21, 177.

Kronenberg, H.M. (2003). Developmental regulation of the growth plate. *Nature* 423, 332–336.

Lejard, V., Brideau, G., Blais, F., Salingcarnboriboon, R., Wagner, G., Roehrl, M.H., Noda, M., Duprez, D., Houillier, P., and Rossert, J. (2007). Scleraxis and NFATc regulate the expression of the pro-alpha1(I) collagen gene in tendon fibroblasts. *J. Biol. Chem.* 282, 17665–17675.

Liu, W., Selever, J., Wang, D., Lu, M.F., Moses, K.A., Schwartz, R.J., and Martin, J.F. (2004). Bmp4 signaling is required for outflow-tract septation and branchial-arch artery remodeling. *Proc. Natl. Acad. Sci. USA* 101, 4489–4494.

Liu, Y., Watanabe, H., Nifuji, A., Yamada, Y., Olson, E.N., and Noda, M. (1997). Overexpression of a single helix-loop-helix-type transcription factor, scleraxis, enhances aggrecan gene expression in osteoblastic osteosarcoma ROS17/2.8 cells. *J. Biol. Chem.* 272, 29880–29885.

Logan, M., Martin, J.F., Nagy, A., Lobe, C., Olson, E.N., and Tabin, C.J. (2002). Expression of Cre recombinase in the developing mouse limb bud driven by a Prx1 enhancer. *Genesis* 33, 77–80.

Massague, J., Seoane, J., and Wotton, D. (2005). Smad transcription factors. *Genes Dev.* 19, 2783–2810.

McLeod, M.J. (1980). Differential staining of cartilage and bone in whole mouse fetuses by alcian blue and alizarin red S. *Teratology* 22, 299–301.

Murchison, N.D., Price, B.A., Conner, D.A., Keene, D.R., Olson, E.N., Tabin, C.J., and Schweitzer, R. (2007). Regulation of tendon differentiation by scleraxis distinguishes force-transmitting tendons from muscle-anchoring tendons. *Development* 134, 2697–2708.

Murtaugh, L.C., Chyung, J.H., and Lassar, A.B. (1999). Sonic hedgehog promotes somitic chondrogenesis by altering the cellular response to BMP signaling. *Genes Dev.* 13, 225–237.

Ogawa, K., Yoshida, A., and Inokuchi, W. (1999). Deltoid contracture: a radiographic survey of bone and joint abnormalities. *J. Shoulder Elbow Surg.* 8, 22–25.

Olsen, B.R., Reginato, A.M., and Wang, W. (2000). Bone development. *Annu. Rev. Cell Dev. Biol.* 16, 191–220.

Ontell, M.P., Sopper, M.M., Lyons, G., Buckingham, M., and Ontell, M. (1993). Modulation of contractile protein gene expression in fetal murine crural muscles: emergence of muscle diversity. *Dev. Dyn.* 198, 203–213.

Ovchinnikov, D.A., Selever, J., Wang, Y., Chen, Y.T., Mishina, Y., Martin, J.F., and Behringer, R.R. (2006). BMP receptor type IA in limb bud mesenchyme regulates distal outgrowth and patterning. *Dev. Biol.* 295, 103–115.

Pai, A.C. (1965a). Developmental genetics of a lethal mutation, Muscular Dysgenesis (Mdg), in the mouse. I. Genetic analysis and gross morphology. *Dev. Biol.* 11, 82–92.

Pai, A.C. (1965b). Developmental genetics of a lethal mutation, Muscular Dysgenesis (Mdg), in the mouse. II. Developmental analysis. *Dev. Biol.* 11, 93–109.

Pogue, R., and Lyons, K. (2006). BMP signaling in the cartilage growth plate. *Curr. Top. Dev. Biol.* 76, 1–48.

Pottorf, J.L., and Lyons, K. (1916). An experimental study of bone growth in the dog. *Anat. Rec.* 10, 234–235.

Pryce, B.A., Brent, A.E., Murchison, N.D., Tabin, C.J., and Schweitzer, R. (2007). Generation of transgenic tendon reporters, ScxGFP and ScxAP, using regulatory elements of the scleraxis gene. *Dev. Dyn.* 236, 1677–1682.

Pryce, B.A., Watson, S.S., Murchison, N.D., Staversky, J.A., Dunker, N., and Schweitzer, R. (2009). Recruitment and maintenance of tendon progenitors by TGF $\beta$  signaling are essential for tendon formation. *Development* 136, 1351–1361.

Reddi, A.H., and Huggins, C. (1972). Biochemical sequences in the transformation of normal fibroblasts in adolescent rats. *Proc. Natl. Acad. Sci. USA* 69, 1601–1605.

Riddle, R.D., Johnson, R.L., Laufer, E., and Tabin, C. (1993). Sonic hedgehog mediates the polarizing activity of the ZPA. *Cell* 75, 1401–1416.

Rot-Nikcevic, I., Reddy, T., Downing, K.J., Belliveau, A.C., Hallgrímsson, B., Hall, B.K., and Kablar, B. (2006). Myf5 $^{−/−}$ :MyoD $^{−/−}$  amyogenic fetuses reveal the importance of early contraction and static loading by striated muscle in mouse skeletogenesis. *Dev. Genes Evol.* 216, 1–9.

Roux, W. (1881). Der kampf der teile im organismus (Leipzig: Engelmann).

Schweitzer, R., Chyung, J.H., Murtaugh, L.C., Brent, A.E., Rosen, V., Olson, E.N., Lassar, A., and Tabin, C.J. (2001). Analysis of the tendon cell fate using Scleraxis, a specific marker for tendons and ligaments. *Development* 128, 3855–3866.

Selever, J., Liu, W., Lu, M.F., Behringer, R.R., and Martin, J.F. (2004). Bmp4 in limb bud mesoderm regulates digit pattern by controlling AER development. *Dev. Biol.* 276, 268–279.

Seo, H.S., and Serra, R. (2007). Deletion of Tgfb2 in Prx1-cre expressing mesenchyme results in defects in development of the long bones and joints. *Dev. Biol.* 310, 304–316.

Shi, Y., and Massague, J. (2003). Mechanisms of TGF- $\beta$  signaling from cell membrane to the nucleus. *Cell* 113, 685–700.

Soriano, P. (1999). Generalized lacZ expression with the ROSA26 Cre reporter strain. *Nat. Genet.* 21, 70–71.

Spagnoli, A., O'Rear, L., Chandler, R.L., Granero-Molto, F., Mortlock, D.P., Gorska, A.E., Weis, J.A., Longobardi, L., Chytil, A., Shimer, K., et al. (2007). TGF- $\beta$  signaling is essential for joint morphogenesis. *J. Cell Biol.* 177, 1105–1117.

Tozer, S., and Duprez, D. (2005). Tendon and ligament: development, repair and disease. *Birth Defects Res. C Embryo Today* 75, 226–236.

Tremblay, P., Dietrich, S., Mericskay, M., Schubert, F.R., Li, Z., and Paulin, D. (1998). A crucial role for Pax3 in the development of the hypaxial musculature and the long-range migration of muscle precursors. *Dev. Biol.* 203, 49–61.

Urist, M.R. (1965). Bone: formation by autoinduction. *Science* 150, 893–899.

Volk, T. (1999). Singling out *Drosophila* tendon cells: a dialogue between two distinct cell types. *Trends Genet.* 15, 448–453.

Wolff, J. (1892). The Law of bone remodeling. *Kirschwald*.

Wozney, J.M., Rosen, V., Celeste, A.J., Mitsock, L.M., Whitters, M.J., Kriz, R.W., Hewick, R.M., and Wang, E.A. (1988). Novel regulators of bone formation: molecular clones and activities. *Science* 242, 1528–1534.

Yamaji, N., Celeste, A.J., Thies, R.S., Song, J.J., Bernier, S.M., Goltzman, D., Lyons, K.M., Nove, J., Rosen, V., and Wozney, J.M. (1994). A mammalian serine/threonine kinase receptor specifically binds BMP-2 and BMP-4. *Biochem. Biophys. Res. Commun.* 205, 1944–1951.

Yoon, B.S., Ovchinnikov, D.A., Yoshii, I., Mishina, Y., Behringer, R.R., and Lyons, K.M. (2005). Bmpr1a and Bmpr1b have overlapping functions and are essential for chondrogenesis in vivo. *Proc. Natl. Acad. Sci. USA* 102, 5062–5067.